J Fluoresc (2008) 18:943–952
DOI 10.1007/s10895-008-0337-y

ORIGINAL PAPER

Rotational Diffusion of Coumarins in Alcohols: A Dielectric Friction Study

B.R. Gayathri · J.R. Mannekutla · S.R. Inamdar

Received: 20 September 2007 / Accepted: 30 January 2008 / Published online: 15 February 2008

Abstract The rotational dynamics of three structurally similar polar molecules viz., coumarin 440, coumarin 151 and coumarin 450 has been studied in alcohols at room temperature using steady-state fluorescence depolarization method and time correlated single photon counting technique. The observed reorientation times of all the three probes are found to be longer than those predicted by Stokes–Einstein–Debye (SED) hydrodynamic theory with stick boundary condition and a deviation towards super-stick behavior is noted. Dielectric friction theories of Nee–Zwanzig and van der Zwan–Hynes, which treat the solute as a point dipole, overestimate the dielectric friction contribution exhibited by all the three coumarins in alcohols. Results are discussed in the light of theoretical models and the possibility of hydrogen bonding between the amino group of the probe molecules and the hydroxyl group of the alcohols.

Keywords Rotational dynamics · Hydrogen bonding · Dielectric friction · Super-stick · Dipole moment

Introduction

The study of various mechanisms by which molecules reorient themselves upon photo-excitation in liquid phase is one of the interesting fields in physical chemistry. The chief motivating factor in carrying out rotational relaxation studies in liquid phase is to understand the solute–solvent interactions, which are important in governing physico-chemical properties of the solutions. Rotational diffusion studies of medium-sized molecules provide a useful means to probe these interactions. The molecules rotating in a liquid experience either mechanical or dielectric friction depending on the nature of the interaction with the neighboring molecules. The mechanical friction between the solute and the solvent depends on the size and shape of the solute molecules and it exists only when either the solute or the solvent is nonpolar or when both of them are nonpolar. The situation is more complicated when a polar solute rotating in a polar solvent polarizes the surrounding solvent medium and the response of the solvent polarization to the solute's rotation not being instantaneous. Under such conditions, the rotating solute molecules experience the dielectric friction besides the mechanical friction. This friction depends on the charge distribution and polarizability of the solute and the solvent molecules. Among various experimental techniques available for the study of solute–solvent interactions, the rotational diffusion studies are highly pragmatic. A number of studies [1–8] involving polar solutes in polar solvents have been carried out and the observed friction, which is proportional to the measured reorientation time, has been conveniently explained as a combination of mechanical and dielectric frictions. If we assume that these two kinds of frictions are separable, then the total friction (ζ_{total}) experienced by the rotating probe molecule is given by [9]

$$\zeta_{total} = \zeta_{mech} + \zeta_{DF} \quad (1)$$

where ζ_{mech} and ζ_{DF} represent the mechanical and dielectric friction contribution, respectively. In general, the mechan-

B. Gayathri
Department of Physics, JSS College,
Dharwad 580 004, India

J. Mannekutla · S. Inamdar (✉)
Laser Spectroscopy Programme, Department of Physics,
Karnatak University,
Dharwad 580 003, India
e-mail: him_lax3@yahoo.com

J. Mannekutla
e-mail: jamphy2002@yahoo.com

ical and dielectric contributions to the friction are not separable as they are interlinked due to electro-hydrodynamic coupling [10–14]. However, detailed investigations of reorientation dynamics have indicated the presence of another source of drag on a rotating probe molecule due to specific interactions such as hydrogen bonding between the solute and the solvent molecules. A solute molecule can form hydrogen bond [15–21] with the solvent molecule depending on the nature of the functional groups on the solute and the solvent. Under such circumstances, the observed reorientation time is longer due to an increase in the effective size of the rotating probe molecule. Nevertheless, such an explanation is only qualitative. Although attempts have been made to quantify specific interactions [16, 17], they are rather rudimentary because it is almost impossible to predict the shape of the hydrogen bonded solute–solvent complex accurately.

The present work deals with the study of rotational dynamics of three structurally similar polar molecules: coumarin 440 (C440), coumarin 151 (C151) and coumarin 450 (C450) in series of alcohols. These molecules possess hydrogen bonding functional groups such as C=O, –NH and $–NH_2$. Normal alcohols are among the most widely used solvents as they not only offer a wide range of viscous and dielectric properties within a homologous series but also have the ability to form hydrogen bonds with the amino and carbonyl groups of the solute molecules. The reorientation time of the solute is therefore expected to reflect on the presence of an additional friction along with the mechanical friction. The aim of the present investigation is to compare the reorientation times of the three probes in order to understand the mechanism underlying the rotational relaxation of these dyes in alcohols.

Experimental

The solutes C440, C450 were procured from Exciton Inc. (USA) and C151 from Lambda Physik Inc. (Germany) and used as received. The alcohols were obtained from Fluka (HPLC) and used without further purification. Figure 1 shows the molecular structures of C440, C151 and C450. The absorption spectra of these probes were recorded using UV–Vis double beam ratio recording spectrophotometer (Hitachi, model U-2800) and fluorescence spectra using fluorescence spectrofluorometer (Hitachi, model F-2000) at 298 K. The solute concentrations were maintained in the range of 10^{-5}–10^{-6} M.

The viscosities of the liquids have been measured by using Schott–Gerate viscometer (model AVS 350, Germany). The unit performs an automated measurement of flow-through times in capillary viscometers. Efflux times have been determined on a digital display to an accuracy of ±0.01 s.

Fig. 1 Molecular structures of **a** C440, **b** C151 and **c** C450

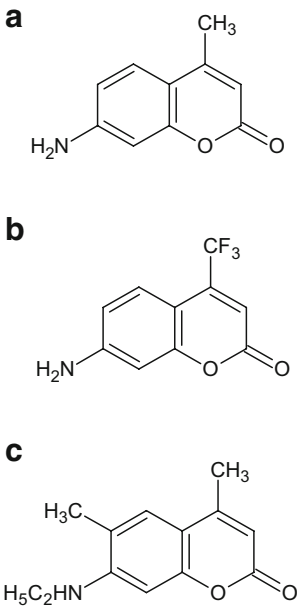

The AVS/S measuring stand was used for optoelectronic sensing of the miniscus. LED in the upper part of the measuring stand generates light in near-infrared range, which is transmitted through a glass cable to measuring levels. Light beam passes through the viscometer and reaches the input end of another light to a receiver in the upper part of the measuring stand. When the liquid miniscus passes through measuring level, light beam is darkened briefly by the optical lens effect of the miniscus and thereafter, intensified for a brief period. This fluctuation of a light beam produces the measuring signal that can be evaluated precisely. Temperature of the bath (Schott–Gerate, model CT 050/2, Germany) was maintained constant within ±01K. Approximately, 5 cm^3 volume of the liquid was taken in the viscometer and allowed to equilibrate to the desired bath temperature for about 10 min. Viscosity of the liquid was calculated using $\eta = tk\rho$ where k is viscometer constant (0.01035 mm^2/s^2), ρ is the density of the liquid and t is efflux time in minutes.

Steady-state fluorescence anisotropies of the probe molecules were measured using fluorescence depolarization technique [22]. For vertically polarized excitation the steady-state fluorescence anisotropy is defined as

$$\langle r \rangle = \frac{I_{||} - GI_{\perp}}{I_{||} + 2GI_{\perp}}, \tag{2}$$

where $I_{||}$ and $I_{\perp}$ are the emission intensities polarized parallel and perpendicular to the excitation polarization, G is an instrumental parameter which corrects for the polarization bias in the detection system and is given by $G = I_{HV}/I_{HH}$, with I_{HV} being the fluorescence intensity when the excitation polarizer is kept horizontal and the emission polarizer vertical, and I_{HH} the fluorescence intensity when both the polarizers are maintained horizontal. The reorien-

tation time τ_r can be obtained from the measured steady-state anisotropy $\langle r \rangle$ and the fluorescence lifetime τ_f using the following relation

$$\tau_r = \frac{\tau_f}{\left[\left(\frac{<r_0>}{<r>}\right) - 1\right]} \quad (3)$$

where r_0 is the limiting anisotropy when all the rotational motions are frozen. In the present study, r_0 values were measured in glycerol (Fluka) at 213 K. The probes were excited at 370 nm and the emission was monitored in the range of 400 to 500 nm.

Fluorescence lifetimes of the solutes were determined using time correlated single photon counting (TCSPC) technique, described elsewhere [23]. The 370 nm second harmonic light pulses were derived from the output of a tunable Ti-sapphire femtosecond laser (Coherent, Mira) with repetition rate of 3.8 MHz. The emission was collected with a resolution of 4 nm at magic angle through a monochromator equipped with a holographic grating with 1,200 grooves/mm. The TCSPC system with thermoelectrically cooled Hamamatsu photomultiplier tube (model H7422) detector has been obtained from Edinburg Instruments (LifeSpec-Red). The instrument response function (IRF) of TCSPC system is ~180 ps. The fluorescence decays were deconvoluted from the IRF using the software F 900.

Results and discussion

SED hydrodynamic theory [16, 24, 25] relates the rotational reorientation time τ_r of a sphere in a continuous homogeneous fluid to the macroscopic viscosity, η of the solvent. According to this theory, the reorientation time, τ_r of a rotating probe molecule is given by

$$\tau_r = \frac{\eta V f C}{kT} \quad (4)$$

where V, T and k, respectively, represent the volume of the rotating species, absolute temperature and Boltzmann constant. The parameter f is the shape factor introduced by Perrin [26] to take care of the non-spherical shape of the solute molecule. The constant C represents the extent of coupling between the rotating probe molecule and the solvent molecules. For a prolate molecule f_{stick} is given by [2]

$$f_{stick} = \frac{2}{3}\frac{1-\rho^4}{\left[\frac{(2-\rho^2)}{(1-\rho^2)^{\frac{1}{2}}}\rho^2 \ln\frac{1+(1-\rho^2)^{\frac{1}{2}}}{\rho}\right] - \rho^2} \quad (5)$$

where ρ is the ratio of semi-major axis (a) to the semi-minor axis (b).

When the size of the rotating probe molecule is much bigger than that of the solvent molecule, the parameter C= 1, which represents the stick boundary condition. In the stick limit, it is assumed that the first layer of the solvent molecules encircling the solute sticks to the solute and there is no relative velocity between them. However, when the probe molecule is of comparable size or smaller than the solvent molecule the value of C is in the range $0<C<1$, which is known as slip boundary condition. The shape factor (f) and the coupling parameter (C) were estimated using semi-major and semi-minor axes of the probe molecule. The value of C for slip boundary conditions can be determined from the Tables of Hu and Zwanzig [27]. The value of f_{stick} can be calculated using Eq. 5, and the rotational reorientation time can be evaluated using Eq. 4.

The van der Waals volumes (V) of C440, C151 and C450 were estimated using Edward's atomic increment method [28] and found to be 152, 165 and 204 Å^3. The distance between the two farthest atoms of the solute molecule was treated as the major axis [29] whose semi-major axes (a) are 4.15, 4.30 and 5.32 Å, respectively, for C440, C151 and C450. The semi-minor axes (b) of the molecules were determined by equating the ellipsoid volume to the van der Waals volume [30, 31] using the relation $b = \sqrt{3V/4\pi a}$ and are found to be 2.96, 3.03 and 3.03 Å, respectively for C440, C151 and C450. The experimentally determined steady-state anisotropies ($<r>$), fluorescence lifetimes (τ_f) and rotational reorientation times (τ_r) of C440, C151 and C450 are tabulated in Table 1. A typical fluorescence decay curve of C450 in decanol is shown in Fig. 2. The fluorescence lifetimes of these molecules vary in the range of 3.41–4.06 ns (C440), 4.78–5.47 ns (C151) and 3.36–3.92 ns (C450). The limiting anisotropy ($<r_0>$) values for C440, C151 and C450 are 0.372±0.002, 0.362±0.003 and 0.357±0.005, respectively, indicating that the absorption and emission dipoles, form angles of 12.47°, 14.58° and 15.53° with respect to each other. The average values of anisotropies $<r>$, are in the range of 0.005±0.001 to 0.074±0.004, 0.004±0.001 to 0.061±0.003 and 0.005±0.001 to 0.078±0.002 for C440, C151 and C450, respectively. From $<r>$, $<r_0>$ and τ_f the reorientation times were obtained using Eq. 3.

Figure 3 shows the variation of rotational reorientation times (τ_r) with solvent viscosity (η) for all the three coumarins, wherein it is seen that τ_r increases linearly with η from methanol to decanol in all the cases. Also it is interesting to note that τ_r values were found to be greater than those predicted by the SED hydrodynamic theory with stick boundary condition. Further, the plot of τ_r vs. η (Fig. 4) of all the molecules under study in series of alcohols is found to be almost similar with trivial variations. This may be attributed to the similarity in the basic structures of these probes. The marginal difference in the

Table 1 Steady-state anisotropy $\langle r \rangle$, fluorescence lifetime (τ_f) and rotational reorientation time (τ_r) of coumarin molecules in alcohols

Solvent	η (mPa s)	Coumarin 440			Coumarin 151			Coumarin 450		
		$\langle r \rangle$	τ_f (ns)[a]	τ_r (ps)	$\langle r \rangle$	τ_f (ns)[a]	τ_r (ps)	$\langle r \rangle$	τ_f (ns)[a]	τ_r (ps)
Methanol	0.55	0.005±0.001	3.90	53±8	0.004±0.001	5.10	57±9	0.005±0.001	3.84	55±9
Ethanol	1.08	0.008±0.001	3.73	82±10	0.007±0.001	5.11	101±12	0.009±0.001	3.69	96±11
Propanol	1.96	0.016±0.001	3.75	168±15	0.016±0.002	4.97	230±19	0.017 + 0.001	3.67	184±15
Butanol	2.59	0.022±0.002	4.06	255±21	0.018±0.002	5.23	274±23	0.025±0.002	3.46	260±22
Pentanol	3.55	0.030±0.002	3.81	333±33	0.023±0.002	5.10	346±34	0.031±0.002	3.57	340±33
Hexanol	4.59	0.033±0.001	3.68	358±31	0.028±0.002	5.25	440±38	0.038±0.002	3.46	412±36
Heptanol	5.87	0.043±0.004	3.41	445±35	0.035±0.003	5.39	577±43	0.046±0.001	3.36	498±37
Octanol	7.61	0.058±0.002	3.76	695±62	0.042±0.002	5.47	718±64	0.058±0.003	3.61	700±62
Nonanol	9.57	0.069±0.002	3.44	783±65	0.052±0.003	4.95	830±70	0.076±0.001	3.60	973±82
Decanol	11.78	0.074± 0.004	3.74	928±60	0.061±0.003	4.78	969±71	0.078±0.002	3.92	1095±80

[a] The error in the fluorescence lifetime is <10%

structural volumes of C440 and C151 is expected to result in almost similar reorientation times. The structure of C450 is about 20–25% larger compared to C440 and C151 with additional non-polar functional groups $-CH_3$ and $-C_2H_5$ at sixth and seventh positions, respectively. The contribution of these additional groups is observed to lead to a sluggish rotational motion and consequently longer reorientation times for C450. The experimental results (Fig. 4) also indicate that C151 is rotating slower than C440 and C450 in alcohols. However, in comparison to C440 and C151, the probe C450 exhibits a relatively slower rotation in higher alcohols. It may also be noted that the stick contribution increases from methanol to decanol in all the three cases. The calculated mechanical contribution amounts to 48%, 50% and 71% of the observed friction for C440, C151 and C450, respectively. The normalized reorientation time τ_r/η, calculated for solvents from methanol to octanol, are found to be 84, 93 and 88 ps/mPa s for C440, C151 and C450, respectively. It is interesting to note that C151 has longer

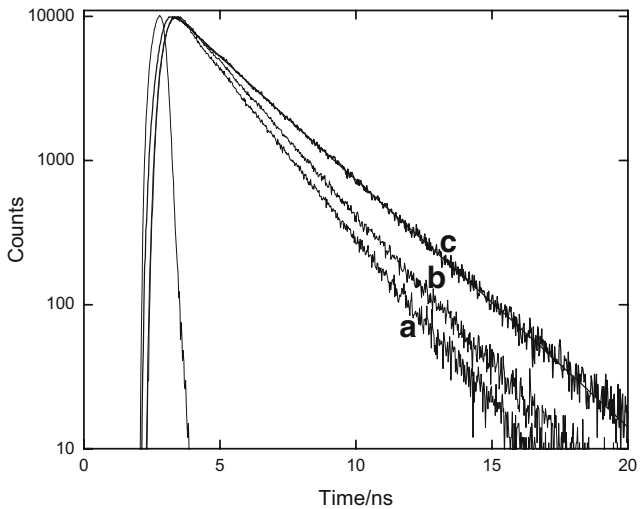

Fig. 2 Typical fluorescence decay curves of **a** C440, **b** C450 and **c** C151 in decanol

diffusion time even though its volume lies in between those of C440 and C450.

Considering the deviations of the experimental results of these molecules from the predictions of the SED theory and the observed super-stick behavior it becomes imperative to check for the influence of dielectric friction, if any. Various methods for calculating the dielectric friction contribution have been proposed and considerable experimental and computational efforts have been expended in testing these theories [9, 32–36]. The deviations of the experimental results from the SED predictions have been explained qualitatively using different theories of dielectric friction. Amongst these, few are classified as continuum theories wherein solvent is characterized by a frequency dependent dielectric constant. Nee–Zwanzig (NZ) [37] and van der Zwan–Hynes (ZH) [38] continuum models have been frequently used to calculate the dielectric friction contribution. NZ theory assumes that the solute is a point dipole located inside a spherical cavity of radius a_0 and the solvent is treated as a continuous dielectric medium characterized by zero frequency and high frequency dielectric constants (ε_0) and (ε_∞) respectively. According to this model the contribution due to dielectric friction is given by

$$\tau_{DF} = \frac{\mu_e^2}{9a_0^3kT}\frac{(\varepsilon_\infty+2)^2(\varepsilon_0-\varepsilon_\infty)}{(2\varepsilon_0+\varepsilon_\infty)^2}\tau_{D,} \qquad (6)$$

where τ_D is the Debye relaxation time of the solvent and μ_e is the excited state dipole moment.

The magnitude of the dielectric friction contribution to the rotational reorientation time (τ_r) crucially depends on the dipole moment of the solute in the excited state. The ground (μ_g) and the excited state (μ_e) dipole moments of the present probes were determined by solvatochromic shift method [39] at 298 K in binary solvent mixture comprising of dimethyl sulphoxide (DMSO) and water at different proportions. The absorption and fluorescence spectra of

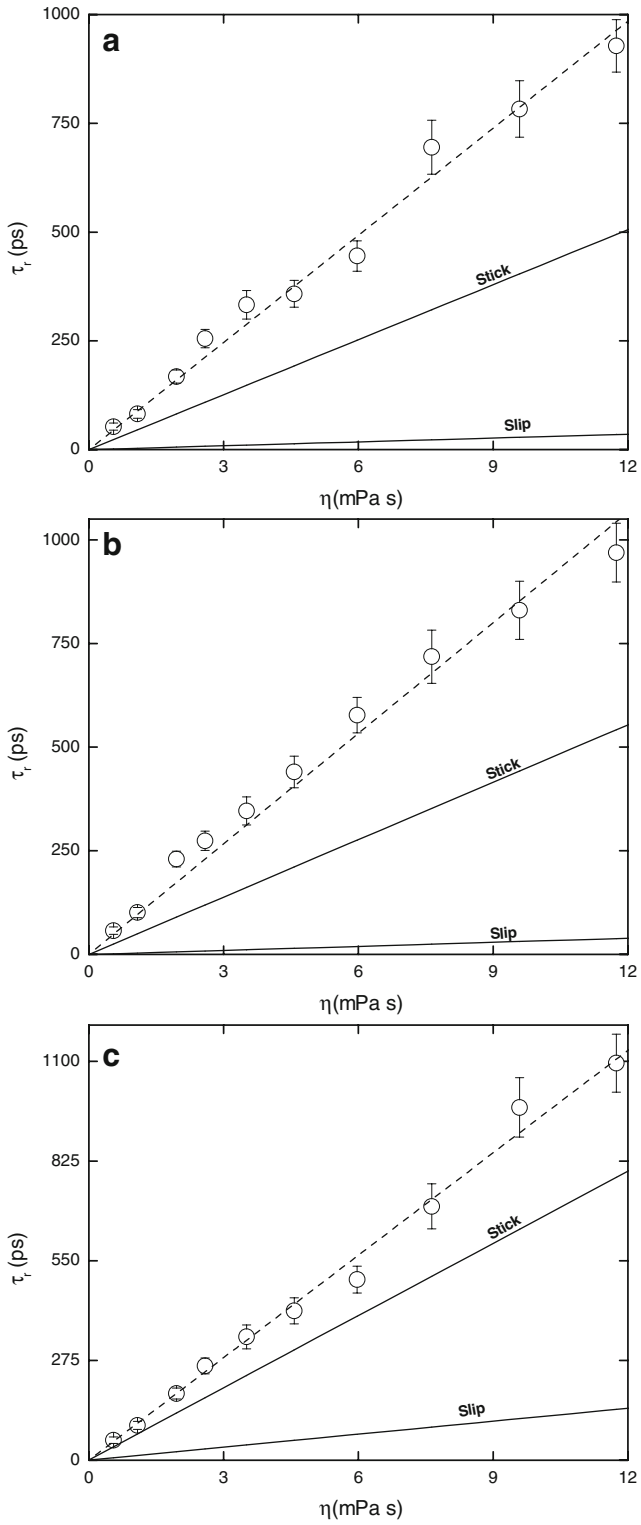

Fig. 3 Plots of rotational reorientation time (τ_r) as a function of viscosity (η) of the solvent in case of **a** C440, **b** C151 and **c** C450. *Solid lines* the theoretical stick (*upper*) and slip (*lower*) lines. *Dashed lines* through the points (*circles*) with *error bars* represents the experimental line

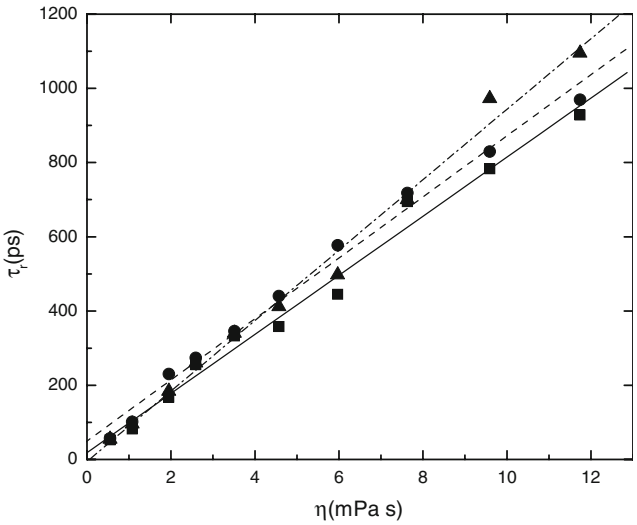

Fig. 4 The plots of the rotational reorientation time vs. viscosity of all the three probes. *Solid line* through the points (*square*), *dashed lines* through the points (*circle*) and *dash dot lines* through the points (*triangle*) represents the rotational reorientation times of C440, C151 and C450 respectively

these coumarins in one of the compositions of binary mixture is shown in Fig. 5. The refractive indices of the solvent mixtures were measured using Abbe's refractometer (ATAGO-3T, Japan) and the dielectric constant ε_0 and Debye relaxation time τ_D were obtained from the literature [7]. The static and dielectric parameters used in the present work are listed in Table 2. The experimentally measured μ_g and μ_e of C440, C151 and C450 were used for the evaluation of dielectric friction, and are tabulated in Table 3 along with the estimated values from Austin model 1 (AM1) method.

Two values of a_0 were used in the NZ model to calculate the contribution due to dielectric friction. One set of values of the cavity radii were obtained from van der Waals volume by treating the solute as a sphere which were found to be a_0=3.37, 3.46 and 3.71 Å whereas, another set of values were taken from the radii equal to half the length of the long axes whose values are, a_0=4.15, 4.30 and 5.32 Å for C440, C151 and C450, respectively. These two values of a_0 for a given molecule represent two extreme limits that can be used to calculate the dielectric friction contribution. The τ_{DF} contribution from the experimentally measured reorientation time was estimated using the relation:

$$\tau_{DF} = \tau_r^{obs} - \tau_r^{stick}, \tag{7}$$

where τ_r^{obs} is the experimentally measured rotational reorientation time and τ_r^{stick} is the theoretical rotational reorientation time according to the SED model. The dielectric friction contribution τ_{DF} calculated using Eq. 6 and those estimated using Eq. 7 are shown as function of A in Fig. 6, where, $A = (\varepsilon_\infty + 2)^2(\varepsilon_0 - \varepsilon_\infty)\tau_D \Big/ (2\varepsilon_0 + \varepsilon_\infty)^2$.

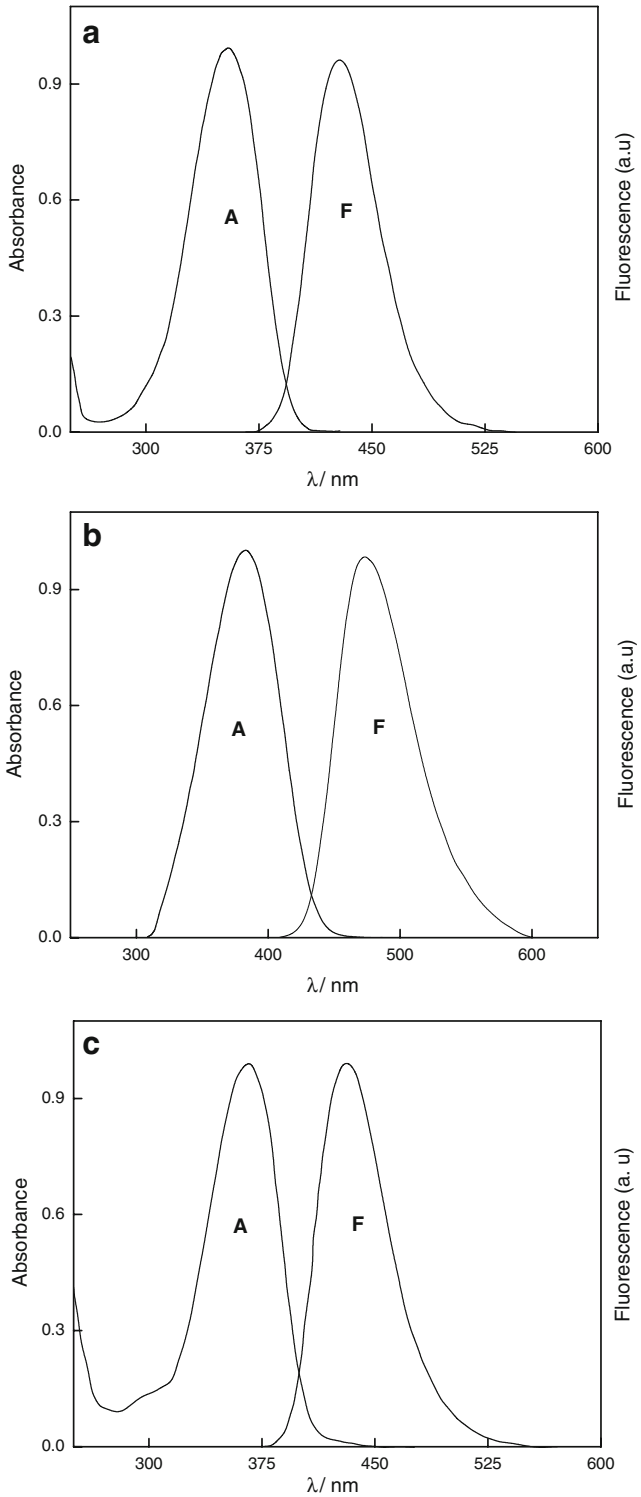

Fig. 5 The absorption and fluorescence spectra of **a** C440, **b** C151 and **c** C450 in one of the compositions of binary mixture

It is evident from Fig. 6, that NZ model overestimates the dielectric friction contribution for both the values of a_0. The excited state dipole moments obtained from the slopes of the experimental plots are tabulated in Table 4. Based on the excited state dipole moments of the coumarins (Table 3),

Table 2 The static and dielectric parameters of the solvents used in the study

Solvent	Dielectric constant		$\tau_D$in picoseconds
	ε_0	ε_∞	
Methanol	33.7	1.77	56
Ethanol	24.3	1.85	139
Propanol	20.6	1.92	362
Butanol	17.4	1.96	482
Pentanol	14.8	1.99	727
Hexanol	13.0	2.01	974
Heptanol	11.3	2.03	1,130
Octanol	9.8	2.04	1,350
Nonanol	9.0	2.05	1,495
Decanol	8.0	2.07	1,639

ε_0 and τ_D are taken from the reference [7]
ε_∞ is taken as the square of the refractive index (n)

the dielectric friction experienced by the probes is expected to be in the order $\tau_{DF}^{450} > \tau_{DF}^{440} > \tau_{DF}^{151}$. However, since the dipole moments obtained for the two values of cavity radius are found to be in the order of $\mu_e^{450} > \mu_e^{151} \approx \mu_e^{440}$, the experimentally observed trend i.e., $\tau_{DF}^{450} > \tau_{DF}^{151} \approx \tau_{DF}^{440}$, is not surprising.

The magnitude of the dielectric friction contribution, according to ZH model, depends on the dipole moment of the solute molecule in the excited state (μ_e) and also on the difference between the ground and excited state dipole moments ($\Delta\mu$) of the solute molecule. The semi-empirical model proposed by ZH [38] relates the dielectric friction experienced by a solute in a solvent to the Stokes shift and solvation time, τ_s, given by

$$\tau_{DF} = \frac{\mu_e^2 hc\Delta\nu}{(\Delta\mu)^2 6kT}\tau_s, \tag{8}$$

where h is the Planck's constant and c the velocity of light. In this approach the Stokes shift $\Delta\nu$ (the difference in energy between the zero-zero transition for absorbance and the zero–zero transition for fluorescence) and the solvation time

Table 3 Ground and excited state dipole moments of the solutes under study

Solute	μ_g (D)	μ_e (D)	$\Delta\mu$ (D)
Coumarin 440	6.03[a]	8.19[a]	1.44[a]
	4.23[b]	7.20[b]	2.97[b]
Coumarin 151	6.04[a]	11.27[a]	5.23[a]
	5.70[c]	11.00[c]	5.30[c]
Coumarin 450	3.63[b]	6.88[b]	3.25[b]
	5.62[b]	8.58[b]	3.16[b]

[a] Measured from AM1 method [50]
[b] Measured from Stokes shift in binary solvent mixture
[c] Measured from AM1 method [51]

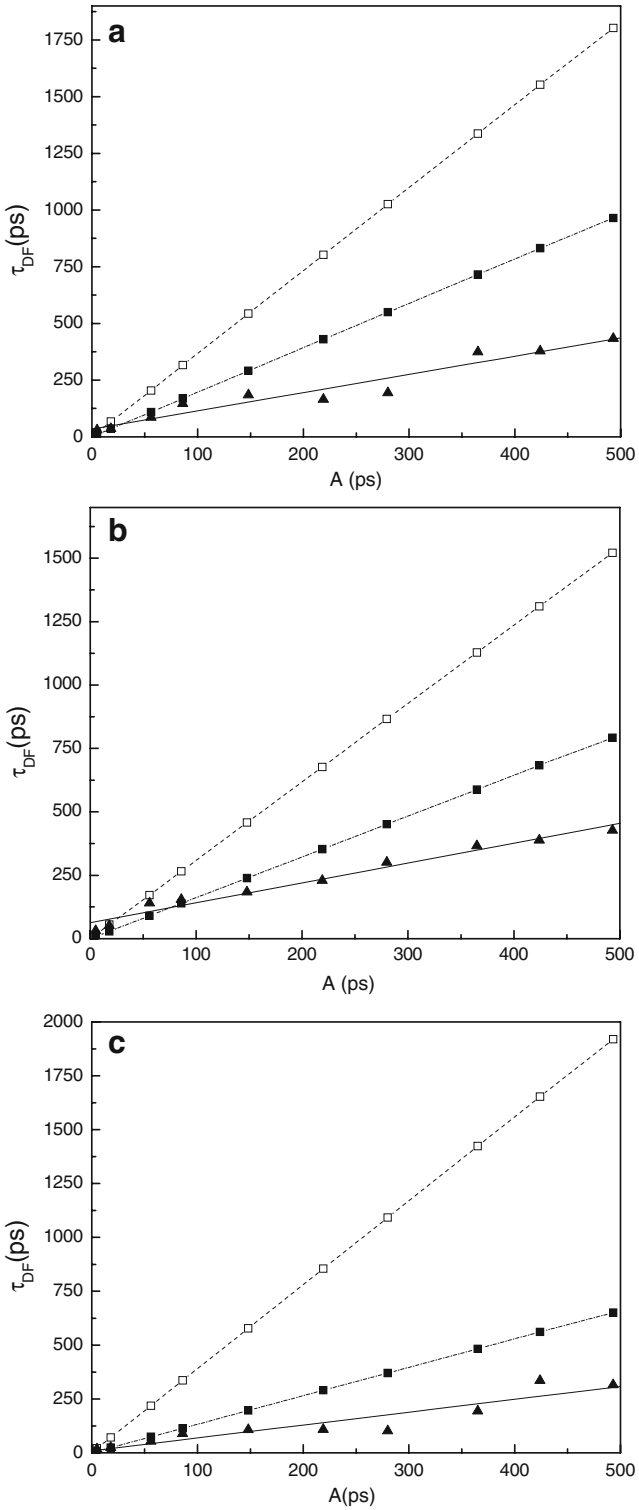

◀**Fig. 6** Rotational reorientation time due to dielectric friction, τ_{DF}, plotted as a function of *A*. *Dashed lines* through the points (*open square*) correspond to the reorientation time due to dielectric friction calculated using cavity radius (a_o) obtained from van der Waals volume determined by Edward's atomic increment method. The *dashed dot lines* through the points (*filled square*) correspond to the reorientation time due to dielectric friction calculated using cavity radius equal to half the length of the major axis. *Solid lines* through experimentally observed points (*triangle*) are obtained by linear least squares fit

τ_s (the correlation time for the temporal evolution of the fluorescence spectrum) is used to gauge the magnitude of the dielectric friction [40]. Studies on solvation dynamics have indicated that the solvation time is approximately related to the solvent longitudinal relaxation time by $\tau_L = \tau_D(\varepsilon_\infty/\varepsilon_0)$ and is relatively independent of the solute properties. Hence, τ_L can be used in place of τ_s.

The dielectric friction contribution was estimated by employing ZH model (Eq. 8). The experimentally measured dielectric friction contribution was obtained as in case of NZ model using Eq. 7. The values of the dielectric friction contribution τ_{DF} thus obtained from theory and experiment are plotted as a function of $\Delta\nu\tau_L$ (Fig. 7). The values of $\mu_e^2/(\Delta\mu)^2$ determined from the slopes of the experimental plots are presented in Table 5 along with the theoretical values. According to the ZH model, based on the theoretically calculated $\mu_e^2/(\Delta\mu)^2$ values and Stokes shifts (the typical values of Stokes shift are 4,799, 5,158 and 4,178 cm^{-1} for C440, C151 and C450, respectively), the expected order of dielectric friction contribution in the case three coumarins is $\tau_{DF}^{440} > \tau_{DF}^{450} > \tau_{DF}^{151}$. But, the observed trend is $\tau_{DF}^{440} > \tau_{DF}^{151} > \tau_{DF}^{450}$.

The super-stick behavior observed for all the coumarins in alcohols suggests the importance of inherent properties of these molecules in determining the rotational reorientation times. The functional group, its position along with the charge on the solute molecule and the nature of the surrounding medium will influence the rotational reorientation time of the solute to a large extent. It has been reported [19] that 1,4-dioxo-3,6-diphenyl-pyrrolo[3,4-c] pyrrole (DPP) with two –NH groups was found to rotate two to three times slower than 2,5-dimethyl-1,4-dioxo-3,6-diphenylpyrrolo[3,4-c] pyrrole (DMDPP), which contains two N–CH_3 groups in

Table 4 Excited state dipole moments obtained from the slopes of experimental plots of τ_{DF} vs *A*

Solute	μ_e (*D*) experimental
Coumarin 440	3.37[a]
	4.6[b]
Coumarin 151	3.46[a]
	4.8[b]
Coumarin 450	3.36[a]
	5.79[b]

[a] For cavity radius calculated from van der Waals atomic increment method

[b] For cavity radius calculated by taking half the length of the major axis

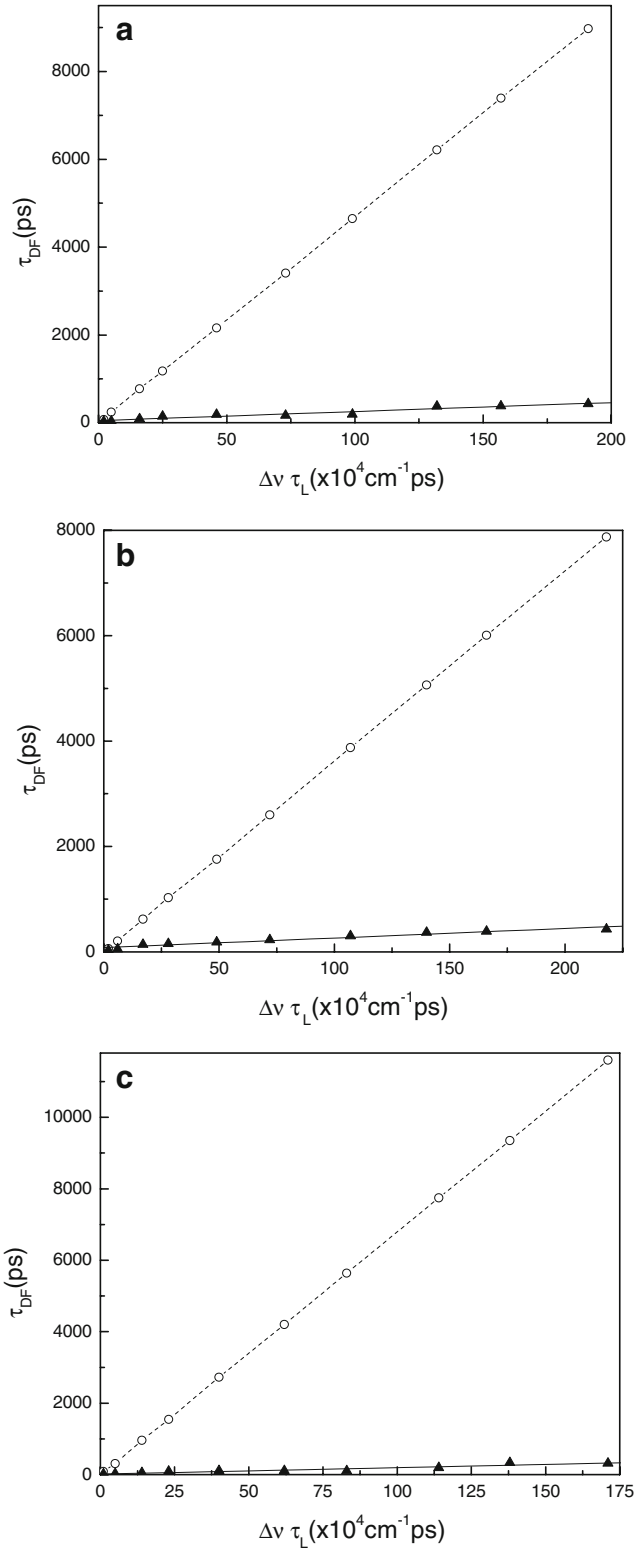

Fig. 7 The rotational reorientation time due to dielectric friction (τ_{DF}) of coumarins is shown as a function of $\Delta\nu\ \tau_L$. *Dashed lines* through the points (*circle*) represent calculated reorientation times following van der Zwan–Hynes model. *Solid lines* through the experimentally observed points (*triangle*) are obtained by linear least squares fit

Table 5 Values of $\frac{\mu_e^2}{(\Delta\mu)^2}$ obtained from the slopes of the experimental plot of τ_{DF} vs $\Delta\nu\tau_L$ and theoretical values taken from Table 2

Solute	$\frac{\mu_e^2}{(\Delta\mu)^2}$	
	Experimental	Theoretical
Coumarin 440	0.26	14.38[a]
Coumarin 151	0.22	4.64[a], 4.31[b]
Coumarin 450	0.22	7.37[c]

[a] Values of μ_e and $\Delta\mu$ are taken from the reference [50]
[b] Values of μ_e and $\Delta\mu$ are taken from the reference [51]
[c] By taking the ratio of $\frac{\mu_e^2}{(\Delta\mu)^2}$ using the values measured from Stokes shift

alcohols. Further DPP exhibited the super-stick behaviour. This super-stick behaviour of DPP was ascribed to the strong hydrogen bonding between the –NH group of DPP and the surrounding solvent molecules. The solute–solvent hydrogen bonding may simply be regarded as an additional friction to the bulk viscosity that slows down the rotational motion of the solute. The additional frictional forces and the specific solute–solvent interactions lead to a deviation from the stick to the super-stick behaviour. A strong hydrogen bonding will lead to the formation of solute–solvent complexes of well-defined stoichiometry. Such larger species consisting of the concerted cluster of solvent molecules and the hydrogen-bonded superstructure can persist in solution for fairly long time and will rotate more slowly than a bare solute molecule. Forming and breaking of hydrogen bonds occurring faster than the probe rotation will provide a channel for dissipation of rotational energy giving rise to additional friction [41]. Based on these facts it has been concluded that the observed deviations from the SED model were largely due to solvent attachment via hydrogen bonding to the solute and consequential increase in the effective volume of the rotating species. It has also been suggested that the rate of forming and breaking of hydrogen bonds is an important parameter which is responsible for the rate limiting process for the unusually longer relaxation times noted in alcohols [42–44].

The size effects were not observed in the present study because the hydrodynamic volume of the probe molecule (solute–solvent complex) increases considererably compared to the size of solvent molecules and thus reorientation times close to stick boundary condition were observed as noted for DPP in decanol and ethylene glycol (EG) solvents [21] due to the interaction between the –NH group of the solute and –OH group of the solvents. This study also prove that the rotating probe molecule experiences more friction as the size of the solute–solvent complex increases. Further in the case of DMDPP in decanol and EG the size effects were observed because of the weakly interacting carbonyl groups of the probe with both the solvents. The rotational dynamics of these two structurally similar non-polar probes in hydrogen bonding solvents thus strongly

supports our observed results. Wiemers and Kauffman [45] have measured the rotational diffusion time of diphenylbutadiene (DPB) and 4-(hydroxymethyl) stilbene (HMS) in series of alcohols in order to examine attractive and repulsive contributions to the rotational diffusion time. The observed differences in the rotational diffusion times suggest that specific hydrogen bonding interactions between HMS and the solvent are responsible for significant solvent friction.

Rotational reorientation times close to stick limit for the probes *N*,*N*′-bis(2,5-di-tert-butylphenyl)-3,4,9,10-perylene (BTBP) and 3,5,3‴,5‴-tetramethyl-*t*-butyl-*p*-quinquephenyl (QUI) in alcohols, respectively, were observed by Ben-Amotz and Drake [46], and Roy and Doraiswamy [47]. They attributed this mainly to the sizes of these probes (V_{BTBP}= 733 Å, V_{QUI}=639 Å), which are much larger than the solvent molecules. However, the molecular sizes of the probes in the present study are much smaller than QUI or BTBP; and as such the size effect cannot be attributed to the observed super-stick behavior. In the present study, C151 exhibits slightly longer diffusion time among those of the three probes, although its volume lies in between those of C440 and C450. This extraordinary behavior can be ascribed to the electron withdrawing capacity of the three fluorine atoms on the fourth carbon atom of C151. This makes it a better hydrogen bond donor [48], which is also responsible for the observed slower reorientation time. Similar observations have been reported [49] in the case of C153 having $-CF_3$ group and C102 having $-CH_3$ group at the fourth position. The rotational reorientation time in squalane was found to be 360 ps for C102, whereas for C153 it was found to be 394 ps in the same solvent. This difference in the reorientation times of C153 was ascribed mainly to the presence of $-CF_3$ group. Moreover, the dipole moment of C151 is also found to be less than that of the other two probes. In a comparative study of rotational reorientation times of coumarin 6, coumarin 7 and coumarin 30 in alcohols, in spite of its smaller dipole moment, C7 was found to rotate 20% slower than C6 [8]. The reason behind this being –NH group of C7 forms strong hydrogen bonds with alcohols. Similarly, C151 rotates relatively slower than the other two probes despite having a smaller dipole moment compared to C440 and C450. In the case of C151, in addition to the hydrogen bonding –NH group, the CF_3 group may also be responsible for the slower rotation. It may be noted that C440 has a secondary amino group $-NH_2$ whereas C450 has a primary amino group –NH. The primary amino group is responsible for the formation of stronger hydrogen bond with hydroxyl group of the alcohols. Thus, the observed slower rotational diffusion of C450 in comparison with C440 is due to stronger solute–solvent hydrogen bonding. In addition, C450 is about 25% lager in size than C440, which will contribute additional mechanical friction especially in nonanol and decanol owing to its solvent-solute size ratio.

Conclusions

Rotational dynamics of C440, C151 and C450 were studied in series of alcohols and the observed rotational reorientation times are found to be longer than the stick limit calculated using SED model. It is interesting to note that C151, with a size lying between that of C440 and C450, rotates slower than the other two molecules. General deviation of the observed reorientation times from the SED theoretical estimations are attributed to the formation of strong hydrogen bonds between amino groups of the probe molecules and hydroxyl group of the alcohols. The rotating probe molecule experiences more friction as the size of the solute–solvent complex increases. However, the nature of the functional group on the solute molecule plays an important role in forming a stable solute-solvent complex which in turn hinders the probe rotation. The weak hydrogen bonds that may also be formed between the carbonyl group of the solute and the hydroxyl groups of the solvent molecules will add further to the slower rotation of these molecules. Dielectric friction theories of NZ and ZH, which treat the solute as a point dipole, overestimate the dielectric friction contribution, exhibited by all the three coumarins in alcohols. Despite the uncertainties involved in the values of dipole moments and cavity radius, reasonable agreement between theory and experiment is observed.

Acknowledgement The authors are grateful to Dr. P.K. Gupta, RRCAT, Indore, for providing TCSPC facility. The funding in the form of a Major Research Project by the University Grants Commission (UGC), New Delhi, is gratefully acknowledged. One of the authors (BRG) is thankful to UGC for a fellowship under Faculty Improvement Program and to the management of JSS. College, Dharwad for the support and encouragement. JRM thanks CSIR, New Delhi, for a Senior Research Fellowship under a Major Research Project.

References

1. Kivelson D, Spears KG (1985) Dielectric friction as a source of rotational drag on charged noncentrosymmetric molecules. J Phys Chem 89:1999–2001
2. Philips LA, Webb SP, Clark JH (1985) High Pressure studies of rotational dynamics: the role of dielectric friction. J Chem Phys 83:5810–5821
3. Gudgin EF, Templeton, Kenney-Wallace GA (1986) Picosecond laser spectroscopic study of orientational dynamics of probe molecules in dimethylsulfoxide-water system. J Phys Chem 90:2896–2900
4. Gudgin Templeton EF, Kenney-Wallace GA (1986) Correlation between molecular reorientation dynamics of ionic probes in polar fluids and dielectric friction by picosecond modulation spectroscopy. J Phys Chem 90:5441–5448
5. Kenney-Wallace GA, Paone S, Kalpouzos C (1988) Femtosecond laser spectroscopy and dynamics of solvation in liquids and electrolytes, Faraday Discussion. Chem Soc 85:185–198
6. Simon JD, Thompson PA (1990) Spectroscopy and rotational dynamics of oxazine 725 in alcohols: a test of dielectric friction theories. J Chem Phys 92:2891–2896

7. Dutt GB, Doraiswamy S (1992) Picosecond reorientational dynamics of polar dye probes in binary aqueous mixtures. J Chem Phys 96:2475–2491
8. Dutt GB, Raman S (2001) Rotational dynamics of coumains: an experimental test of dielectric friction theories. J Chem Phys 114:6702–6712
9. Hartman RS, Waldeck DH (1994) A test of dielectric models: rotational diffusion of fluorenes in dimethylsulphoxide. J Phys Chem 98:1386–1393
10. Hubbard JB, Onsager L (1977) Dielectric dispersion and dielectric friction in electrolyte solutions. J Chem Phys 67:4850–4857
11. Hubbard JB (1978) Friction on a rotating dipole. J Chem Phys 69:1007–1009
12. Felderhof BU (1983) Dielectric friction on a polar molecule rotating in a fluid. Mol Phys 48:1269–1281
13. Felderhof BU (1983) Dielectric friction on an ion rotating in a fluid. Mol Phys 48:1283–1288
14. Kumar PV, Maroncelli M (2000) The non-separability of "dielectric" and "mechanical" friction in molecular systems: a simulation study. J Chem Phys 112:5370–5381
15. Dutt GB, Ramakrishna G (2000) Temperature-dependent rotational relaxation of nonpolar probes in mono and diols: Size effects versus hydrogen bonding. J Chem Phys 112:4676–4682
16. Fleming GR (1986) Chemical applications of ultra fast spectroscopy. Oxford University Press, London
17. Spears KG, Steinmetz KM (1985) Solvent interactions with anions by reorientation studies of resorufin. J Phys Chem 89:3623–3629
18. Moog RS, Bankert DL, Maroncelli M (1993) Rotational diffusion of coumarin 102 in trifluoroethanol: the case for solvent attachment. J Phys Chem 97:1496–1501
19. Dutt GB, Srivastavoy VJP, Sapre AV (1999) Rotational dynamics of pyrrolopyrrole derivatives in alcohols: does solute-solvent hydrogen bonding really hinder molecular rotation? J Chem Phys 110:9623–9629
20. Dutt GB, Srivastavoy VJP, Sapre AV (1999) Rotational dynamics of pyrrolopyrrole derivatives in glycerol: a comparative study with alcohols. J Chem Phys 111:9705–9710
21. Dutt GB (2000) Rotational dynamics of non-dipolar probes in alkane–alkanol mixtures: microscopic friction on hydrogen bonding and non-hydrogen bonding solute molecules. J Chem Phys 113:11154–11158
22. Lackowicz JR (1983) Principles of fluorescence spectroscopy. Plenum, New York
23. Das K, Jain B, Dube A, Gupta PK (2005) pH dependant binding of chlorine-p6 with phosphatidyl choline liposomes. Chem Phys Lett 401:185–188
24. Debye P (1929) Polar Molecules. Dover, London
25. Kievelson D (1987) Rotational dynamics of small and macro molecules. Springer, Berlin
26. Perrin F (1934) Mouvement Brownien d'un ellipsoide (I). Dispersion diélectrique pour des molécules ellipsoidales.. J Phys Radium 5:497–512
27. Hu CM, Zwanzig R (1974) Rotational friction coefficients for spheroids with the slipping boundary condition. J Chem Phys 60:4354–4357
28. Edward JT (1970) Molecular volumes and the Stokes–Einstein equation. J Chem Educ 47:261–270
29. Dutt GB, Sachdeva A (2003) Temperature-dependent rotational relaxation in a viscous alkane: Interplay of shape factor and boundary condition on molecular rotation. J Chem Phys 118:8307–8314
30. Ben-Amotz, Drake D (1988) The solute size effect in rotational diffusion experiments: a test of microscopic friction theories. J Chem Phys 89:1019–1029
31. Williams AM, Jiang Y, Ben-Amotz D (1994) Molecular reorientation dynamics and microscopic friction in liquids. Chem Phys 180:119–129
32. Alavi DS, Hartman RS, Waldeck DH (1991) A test of continuum models for dielectric friction: Rotational diffusion of phenoxazine dyes in dimethylsulphoxide. J Chem Phys 94:4509–4520
33. Alavi DS, Hartman RS, Waldeck DH (1991) The influence of wave vector dependent dielectric properties on rotational friction: Rotational diffusion of phenoxazine dyes. J Chem Phys 95:6770–6783
34. Hartman RS, Alavi DS, Waldeck DH (1991) An experimental test of dielectric friction models using the rotational diffusion of aminoanthraquinones. J Phys Chem 95:7872–7880
35. Alavi DS, Waldeck DH (1991) A test of hydrodynamics in binary solvent systems: rotational diffusion studies of oxazine 118. J Phys Chem 95:4848–4852
36. Hartman RS, Konitsky WM, Waldeck DH, Chang YJ, Castner EW (1997) Probing solute-solvent electrostatic interactions: rotational diffusion studies of 9,10-disubstituted anthracenes. J Chem Phys 106:7920–7930
37. Nee TW, Zwanzig R (1970) Theory of dielectric relaxation in polar liquids. J Chem Phys 52:6353–6363
38. van der Zwan G, Hynes JT (1985) Time-dependent fluorescence solvent shifts, dielectric friction and nonequilibrium solvation in polar solvents. J Phys Chem 89:4181–4188
39. Nadaf YF, Mulimani BG, Gopal M, Inamdar SR (2004) Ground and excited state dipole moments of some exalite UV laser dyes from solvatochromic method using solvent polarity parameters. J Mol Struct 678:177–181
40. Hartman RD, Waldeck DH (1991) An experimental test of dielectric friction models using the rotational diffusion of aminoanthraquinones. J Phys Chem 95:7872–7880
41. Imeshev G, Khundkar LR (1995) Homogeneous rotational dynamics of a rod like probe in 1-propanol. J Chem Phys 103:8322–8328
42. Garg SK, Smyth CP (1965) Microwave absorption and molecular structure in liquids. The three dielectric dispersion regions of the normal primary alcohols.. J Phys Chem 69:1294–1301
43. Denny DJ, Cole RH (1955) Dielectric properties of methanol and methanol-1-propanol solutions. J Chem Phys 23:1767–1772
44. Brot C, Magat M (1963) Comment on "dispersion at millimetre wavelengths in methyl and ethyl alcohols. J Chem Phys 39:841–842
45. Wiemers K, Kauffman JF (2000) Dielectric friction and rotational diffusion of hydrogen bonding solutes. J Phys Chem 104:451–457
46. Ben-Amotz D, Drake JM (1988) The solute size effect in rotational diffusion experiments: a test of microscopic friction theories. J Chem Phys 89:1019–1029
47. Roy M, Doraiswamy S (1993) Rotational dynamics of nonpolar solutes in different solvents: comparative evaluation of the hydrodynamic and quasihydrodynamic models. J Chem Phys 98:3213–3224
48. Dutt GB, Ghanty TK (2003) Rotational dynamics of nonpolar probes in ethanols: how does the strength of solute-solvent hydrogen bond impede molecular rotation? J Chem Phys 119:4768–4774
49. Horng ML, Gardecki JA, Maroncelli M (1997) Rotational dynamics of coumarin 153: time-dependent friction, dielectric friction, and other nonhydrodynamic effects. J Phys Chem A 101:1030–1047
50. McCarthy PK, Blanchard GJ (1993) AM1 study of the electronic structure of coumarins. J Phys Chem 97:12205–12209
51. Tamashiro A, Rodriguez J, Laria D (2001) Equillibrium and dynamical aspects of solvation of coumarin-151 in polar nanoclusters. J Phy Chem 106:215–221